analytical chemistry

Article

Cite This: Anal. Chem. 2017, 89, 12425-12432

pubs.acs.org/ac

Hydrophilic Interaction Liquid Chromatography–Mass Spectrometry Characterization of Gangliosides in Biological Samples

Roman Hájek, Robert Jirásko, Miroslav Lísa, Eva Cífková, and Michal Holčapek*

Department of Analytical Chemistry, Faculty of Chemical Technology, University of Pardubice, Studentská 573, 53210 Pardubice, Czech Republic

Supporting Information

ABSTRACT: The hydrophilic interaction liquid chromatography (HILIC) coupled to a negative-ion electrospray ionization tandem mass spectrometry (ESI-MS/MS) method has been developed for the identification of a wide range of gangliosides in biological samples. Gangliosides consist of a backbone of sphingoid base and a polar oligosaccharide chain containing at least one sialic acid. Gangliosides are extracted by chloroform–methanol–water mixture, where an upper aqueous layer containing gangliosides and other polar lipid subclasses is further purified by C18 solid-phase extraction. The optimization of chromatographic conditions includes the column selection, mobile-phase composition, pH value, buffer type, and concentration with the goal to achieve the best chromatographic resolution and MS sensitivity. The identification of gangliosides and other polar lipids is based on accurate m/z values of $[M-H]^-$ ions and fragment ions as well measured by high-resolution MS. The detailed interpretation of MS/MS spectra enables the generalization of fragmentation pathways, which is then used for the differentiation of *a*, *b*, and *c* series of gangliosides. The structural assignment is further confirmed by agreement with the predicted retention behavior in HILIC mode on the basis of the correlation among the ganglioside retention, the number of saccharide units, and their sequence. The final HILIC/ESI-MS/MS method is applied for the analysis of porcine brain, human kidney, lungs, plasma, and erythrocytes resulting in unambiguous identification of 145 ganglioside species from 19 subclasses, which represents the highest number of reported gangliosides. Moreover, 71 sulfatides and 59 polar phospholipids (phosphatidylserines, phosphatidylinositols, lysophosphatidylinositols, and phosphatidylglycerols) are detected within a 15 min run.

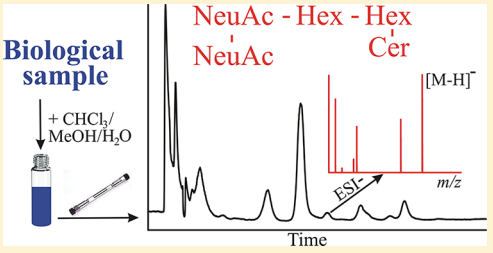

Sphingolipids are one of eight (fatty acyls, glycerolipids, glycerophospholipids, sterol lipids, prenol lipids, saccharolipids, polyketides, and sphingolipids) major lipid categories according to LIPID MAPS classification.[1] This category comprises highly diverse lipid species, where fatty acyls are linked via amide bond to a long chain base or sphingoid. The group of acidic sphingolipids contains gangliosides, which are sphingolipids containing the sphingoid base (ceramide) attached to mono- or polysialylated oligosaccharides. Gangliosides may have a different composition of sphingoid base, N-fatty acyls, and an oligosaccharide part, which results in a large complexity of natural gangliosides. Ceramide moiety can be attached to various sugars: (1) one or more uncharged sugars, such as glucose (Glc) or galactose (Gal), with possible further attachment of other neutral sugars, such as *N*-acetylgalactosamine (GalNAc), *N*-acetylglucosamine (GlcNAc), and fucose (Fuc); (2) ionized functional groups, such as sulfate attached to uncharged sugars or sialic acid residues. Sialic acid is a trivial name used for all derivatives of neuraminic acid,[2] where the most important is *N*-acetylneuraminic acid (NeuAc, SA) and less common is *N*-glycolylneuraminic acid (NeuGc). NeuAc and NeuGc are structurally similar, but they differ significantly in their natural occurrence. NeuAc is present in human unlike NeuGc, which is obtained only from the diet in a limited amount.[2−4] Gangliosides have important biological functions in mammalian cells.[2,5] They are present in almost all human tissues, and they are particularly abundant in neural tissues and extraneural organs, such as the lungs, spleen, and gut as well as in some biological fluids, such as milk.[6−10] Gangliosides are abundant in the central nervous system, and they play important roles in many physiological processes in cells, such as memory control, cell signaling, neuronal recovery, neuronal protection, apoptosis, adhesion, and differentiation.[2,11−15]

Gangliosides are complex lipids, and their analysis is critical for the understanding of their functions in the organism. The sample preparation is a crucial step due to low natural abundances of gangliosides. Typically, modifications of Folch extraction based on chloroform–methanol–water system are used[16] with further purification of upper aqueous phase by solid-phase extraction (SPE) using reversed-phase (RP)[9,17] or anion-exchange[18] modes to remove undesired salts and other contaminants. The extracts of gangliosides can be separated by liquid chromatography (LC)[5,18] using RP[9,18] or HILIC systems[5] and thin-layer chromatography (TLC).[6,19] The identification of gangliosides in biological tissues and fluids is a challenging task, which typically requires the use of tandem mass spectrometry (MS/MS) coupled to chromatographic

Received: August 29, 2017
Accepted: October 23, 2017
Published: October 23, 2017

DOI: 10.1021/acs.analchem.7b03523
Anal. Chem. 2017, 89, 12425−12432

techniques[20,21] or in shotgun configuration without chromatographic separation.[22,23] Negative-ion electrospray ionization (ESI) is the most convenient ionization mode for these acidic sphingolipids.[5,7,8,18,24] The derivatization can improve the sensitivity of gangliosides determination,[25] but it may be difficult to apply laborious derivatization procedure for high-throughput analysis of large series of clinical samples. The combination of mass spectrometry imaging and immunohistochemistry has been applied for multimodal detection of GM2 and GM3 in mice brain.[26] Another application of mass spectrometry imaging for spatial characterization of gangliosides in mice brain is based on the combination of imaging and ion mobility separation.[27]

In this study, the development and systematic optimization of HILIC/ESI-MS/MS method for the analysis of wide range of gangliosides is reported. The main parameters of the chromatographic optimization are the selection of the chromatographic column, the mobile-phase composition including pH value, type and concentration of buffers with the goal to achieve the best chromatographic resolution and also sensitivity with negative-ion ESI-MS detection. The fragmentation behavior of individual ganglioside subclasses in MS/MS mode is studied to elucidate the structure of both oligosaccharide and ceramide parts of ganglioside molecules. The developed method is applied for the analysis of biological samples, such as human kidney, lungs, plasma, erythrocytes, and porcine brain.

EXPERIMENTAL SECTION

Chemicals and Standards. Acetonitrile, methanol (both HPLC/MS grade), chloroform (HPLC grade, stabilized by 0.5−1% ethanol), ammonium formate, ammonium acetate, formic acid, and acetic acid were purchased from Sigma-Aldrich (St. Louis, MO, U.S.A.). Deionized water was prepared with a Milli-Q Reference Water Purification System (Molsheim, France). The standard of total ganglioside extract from porcine brain was purchased from Avanti Polar Lipids (Alabaster, AL, U.S.A.). The porcine brain was obtained from the local farm. Samples of plasma, erythrocytes, and kidney were obtained from the Department of Urology, Palacký University, Faculty of Medicine and Dentistry and University Hospital, Olomouc, Czech Republic. The sample of lungs was obtained from the Regional Hospital of Pardubice, Czech Republic. The study was approved by the hospital Ethical Committee, and patients signed documents giving their informed consent.

Sample Preparation. Two milligrams of total ganglioside extract from porcine brain was dissolved in 1100 μL of chloroform−methanol−water (600:425:75, v/v/v) mixture. Human blood was collected to heparin-lithium tubes and ultracentrifuged to obtain plasma. Samples of human kidney and human lungs were obtained during surgery, immediately frozen, and stored at −80 °C until the sample processing and the analysis. Human kidney, lungs, plasma, erythrocytes, and porcine brain tissue extracts were obtained by chloroform−methanol−water extraction according to Folch method[28] with minor modifications.[16,29,30] Initially, 25 mg of each tissue (human kidney, human lungs, or porcine brain) was cut by scalpel and homogenized in 6 mL of a chloroform−methanol mixture (2:1, v/v) using an ultrasonic bath at 40 °C for 10 min, while human plasma (200 μL) and erythrocytes (200 μL) were homogenized in 3 mL of chloroform−methanol mixture (2:1, v/v) using an ultrasonic bath at 40 °C for 10 min. Then, deionized water (1200 μL for tissues and 600 μL for plasma and erythrocytes) was added, and the mixture was centrifuged at 3000 rpm for 3 min under ambient conditions. The upper aqueous layer containing gangliosides was collected, evaporated by gentle stream of nitrogen to dryness, redissolved in 1 mL of water, and purified by SPE. First, 200 mg of tC18 cartridge (Sep-Pak Vac, 37−55 μm particle size) (Waters, Milford, MA, U.S.A.) was conditioned with 3 × 1 mL of methanol followed by 3 × 1 mL of water. Then, 1 mL of sample dissolved in water was loaded on the column, washed 3 times with 1 mL of water, and finally eluted by 3 × 1 mL of methanol. The eluate was collected, then evaporated by a gentle stream of nitrogen to dryness and redissolved in 500 μL of methanol−water−chloroform (300:150:50, v/v/v) mixture for the HILIC/ESI-MS analysis. The extraction recovery tested for GM3 subclass was 106% for high-level concentration and 103% for low-level concentration.

HILIC/ESI-MS Conditions. All LC experiments were performed on a liquid chromatograph Agilent 1290 Infinity series (Agilent Technologies, Waldbronn, Germany). The final method for the analysis of individual lipid subclasses used the following conditions: Ascentis Si column (150 × 2.1, 3 μm, Sigma-Aldrich), flow rate 0.3 mL/min, injection volume 1 μL, column temperature 40 °C, and mobile-phase gradient as follows—0 min: 87.7% A + 12.3% B; 15 min: 77.9% A + 22.1% B, where phase A was acetonitrile with acetic acid, and phase B was 10 mM aqueous ammonium acetate with pH 6.1 adjusted by acetic acid. The reequilibration time between runs is 15 min. The pH was measured by portable pH meter Checker (Hanna Instruments, Woonsocket, RI, U.S.A.). For all mobile phases used in this work, acetonitrile (phase A) contained the identical amount of formic or acetic acid as used for the pH adjustment of aqueous solution (phase B). The concentration of 10 mM of ammonium formate or ammonium acetate is used for the experimental optimization of the best pH value for the separation of gangliosides. The pH value is adjusted by the addition of formic or acetic acid to aqueous phase and subsequently pH measured by pH meter. The longer gradient was used during the method optimization—0 min: 99.5% A + 0.5% B; 55 min: 75.4% A + 24.6% B and flow rate 0.4 mL/min. Other conditions were identical as for the final method described above.

The following setting of hybrid quadrupole time-of-flight mass spectrometer (micrOTOF-Q, Bruker Daltonics, Bremen, Germany) in ESI mode was used: capillary voltage 2.5 kV, nebulizing gas pressure 1.2 bar, drying gas flow rate 9.3 L/min, and drying gas temperature 210 °C. ESI mass spectra were measured in the range of m/z 50−3000 in the negative-ion mode using the following setting of funnel 1 RF 400 Vpp, funnel 2 RF 400 Vpp, ISCID energy 0 eV, hexapole RF 400 Vpp, quadrupole ion energy 5 eV, low mass 300 m/z, collision cell energy 10 eV, collision RF 600 Vpp, transfer time 80 μs, and prepulse storage 12 μs. MS/MS spectra of up to 4 most abundant ions from the inclusion list were measured after each full MS scan in the data-dependent mode using the scan time of 0.5 s with 0.01 s of interscan time. The total cycle time is 0.51 s. The collision energy ramp was used for the fragmentation starting from m/z 700 as the low mass (collision energy 20 eV) up to m/z 2000 as the high mass (collision energy 70 eV).

The hybrid quadrupole−traveling wave ion mobility−time-of-flight mass spectrometer Synapt G2Si (Waters) in the resolution mode was used for the identification with the following conditions: negative-ion ESI, mass range m/z 50−2000, capillary voltage 2.2 kV, sampling cone 20 V, source offset 90 V, source temperature 150 °C, drying temperature

DOI: 10.1021/acs.analchem.7b03523
Anal. Chem. 2017, 89, 12425−12432

500 °C, cone gas flow 0.8 L/min, drying gas flow 17 L/min, and nebulizer gas flow 4 bar. Leucine enkephaline was used as the lock mass for all experiments. MS/MS experiments were performed on the transfer cell with the collision energy ramp from 20 to 70 eV.

RESULTS AND DISCUSSION

Nomenclature of Gangliosides. The first nomenclature of gangliosides was introduced by Svennerholm[31] and later

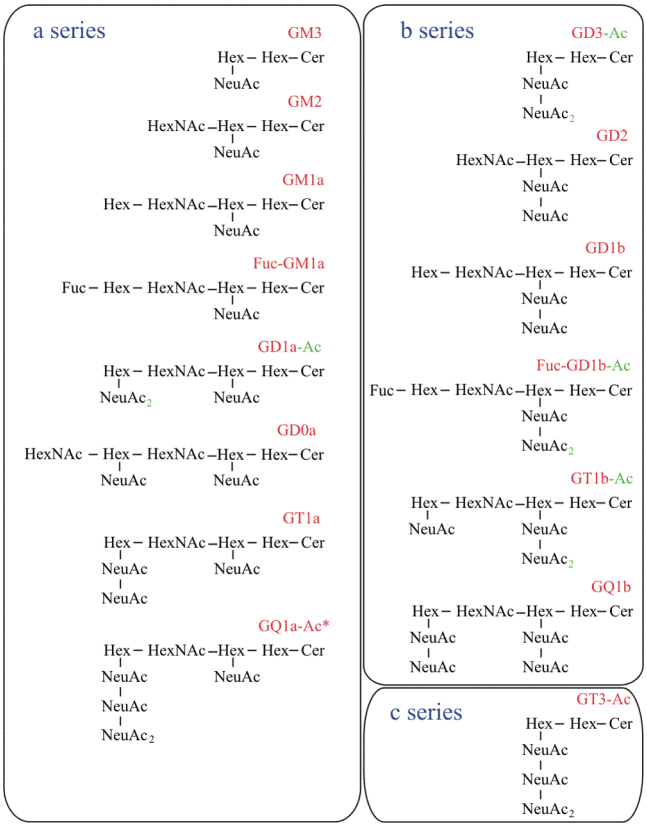

Figure 1. Structures of gangliosides identified in this work. Annotation:[32] the first letter G means ganglioside, the second letter indicates the number of sialic acids (M = mono, D = di, T = tri, and Q = tetra), then the number of neutral saccharide units is calculated as 5−*n*, the series *a* is −Hex(NeuAc)−Hex−Cer, the series *b* is −Hex(NeuAc−NeuAc)−Hex−Cer, and the series *c* is −Hex-(NeuAc−NeuAc−NeuAc)−Hex−Cer. The asterisk (GQ1a−Ac*) means that the structure is not confirmed by MS/MS spectra.

approved by IUPAC.[32] In the shorthand notation system of gangliosides, the first letter G means ganglioside, the second letter indicates the number of sialic acids (M = mono, D = di, T = tri, and Q = tetra), then the number of neutral sugars is calculated as 5−*n* saccharide units, which may be followed by small letter *a*, *b*, or *c* defining the position of sialic acid(s). This notation may be explained on the example of GM1a (see Figure 1), which is ganglioside (G) containing one sialic acid (M), four neutral sugars (*n* = 4, i.e., 5−4 = 1), and the final small letter *a* describes the position of sialic acid. The abbreviation Ac means additional acetylation, for example, in the case of GD1−Ac. The colon-separated numbers (e.g., 36:1) behind ganglioside abbreviations provides the information on the total number of carbon atoms and double bonds (CN:DB) of N-linked fatty acyl and sphingoid base of ceramide part, and this annotation is based on the common assumption of sphingoid base with two

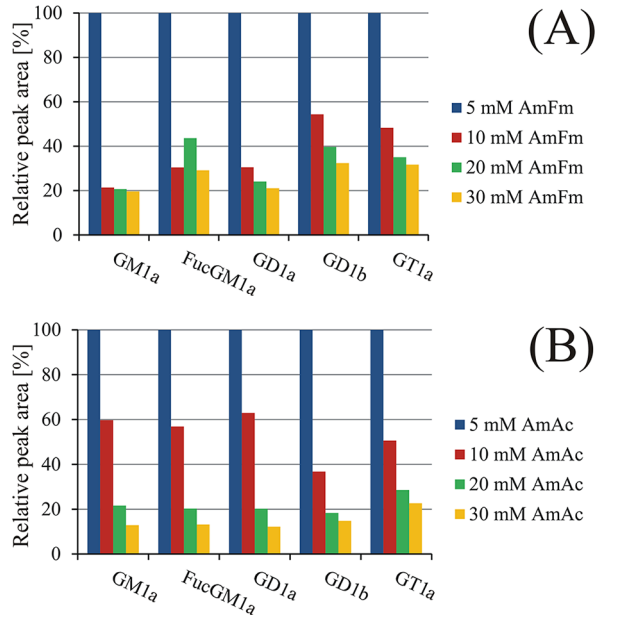

Figure 2. Comparison of relative peak areas vs molar concentrations of (A) ammonium formate (AmFm) and (B) ammonium acetate (AmAc) for major individual gangliosides GM1a 36:1 (RIC of $[M-H]^-$ at m/z 1544.9), Fuc−GM1a 36:1 (RIC of $[M-H]^-$ at m/z 1690.9), GD1a 36:1 (RIC of $[M-H]^{2-}$ at m/z 917.5), GD1b 36:1 (RIC of $[M-H]^{2-}$ at m/z 917.5), and GT1b 38:1 (RIC of $[M-H]^{2-}$ at m/z 1077.0).

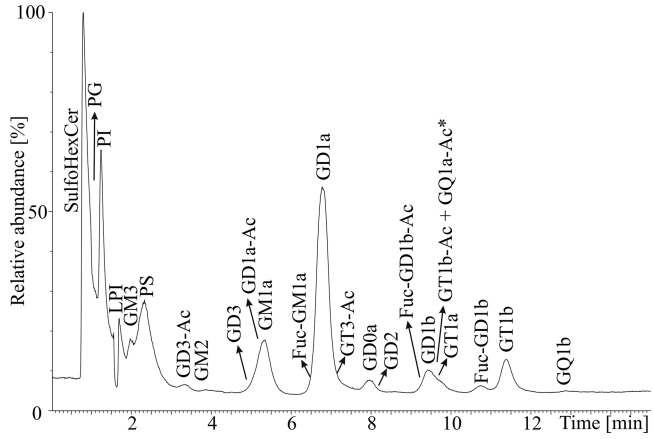

Figure 3. Negative-ion HILIC/ESI-MS total ion current chromatogram of porcine brain extract. Conditions: Ascentis Si column (150 × 2.1, 3 μm, Sigma-Aldrich), flow rate 0.3 mL/min, injection volume 1 μL, column temperature 40 °C, and mobile-phase gradient—0 min: 87.7% A + 12.3% B; 15 min: 77.9% A + 22.1% B, where phase A was acetonitrile with acetic acid, and phase B was 10 mM aqueous ammonium acetate with pH 6.1 adjusted by acetic acid (more details in Experimental Section).

hydroxyl groups and no hydroxylation of *N*-acyl. In the case of the presence of additional hydroxyl on the ceramide part without any specification of its position, the OH in parentheses is space separated and placed behind the ceramide DB number.

Dissociation Equilibria of Gangliosides. In general, ganglioside molecules may be multiply charged depending on the pH value and the number of sialic acids containing a carboxylic functional group, which may be easily deprotonated to form carboxylate. The first step in the optimization of HILIC conditions is the selection of an optimal pH value, where all

DOI: 10.1021/acs.analchem.7b03523
Anal. Chem. 2017, 89, 12425−12432

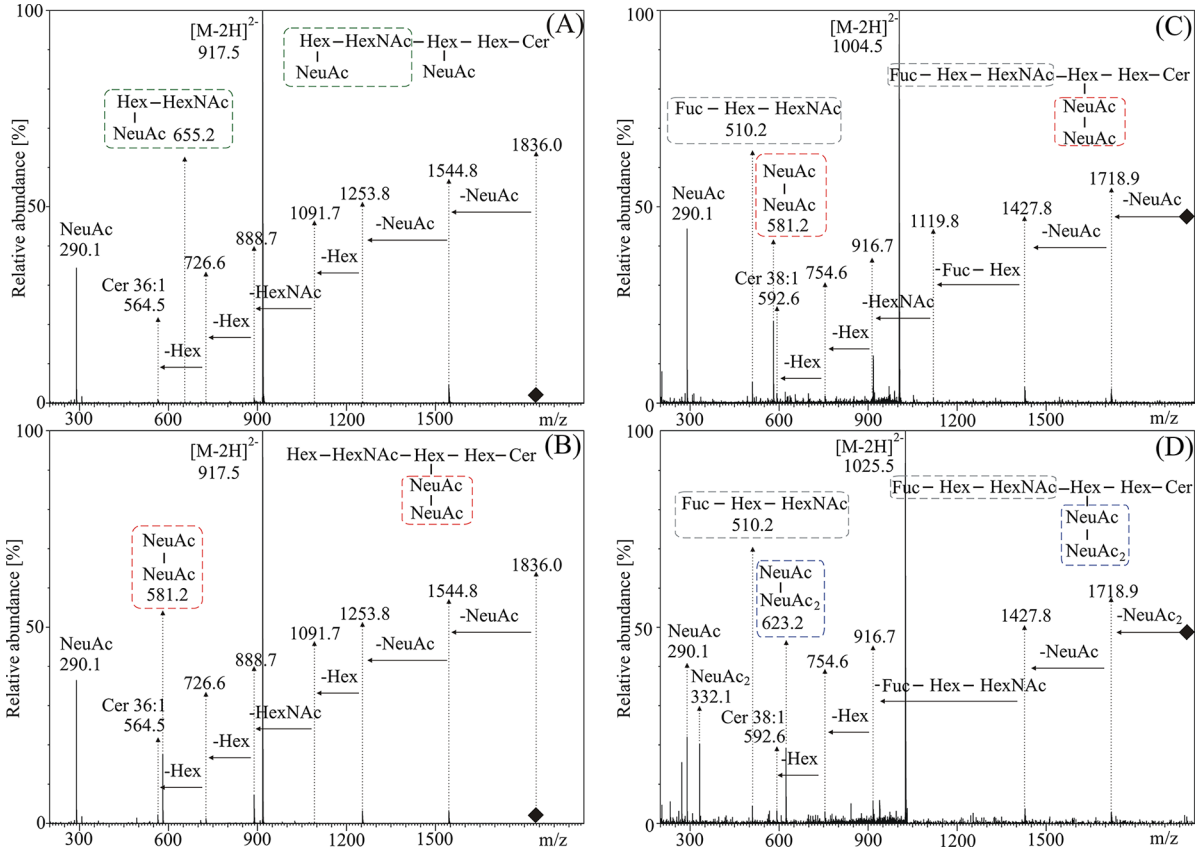

Figure 4. HILIC/ESI-MS/MS fragmentation behavior of (A) $[M-2H]^{2-}$ ion of GD1a 36:1 at m/z 917.5, (B) $[M-2H]^{2-}$ ion of GD1b 36:1 at m/z 917.5, (C) $[M-2H]^{2-}$ ion of Fuc−GD1b 38:1 at m/z 1004.5, and (D) $[M-2H]^{2-}$ ion of Fuc−GD1b−Ac 38:1 at m/z 1025.5.

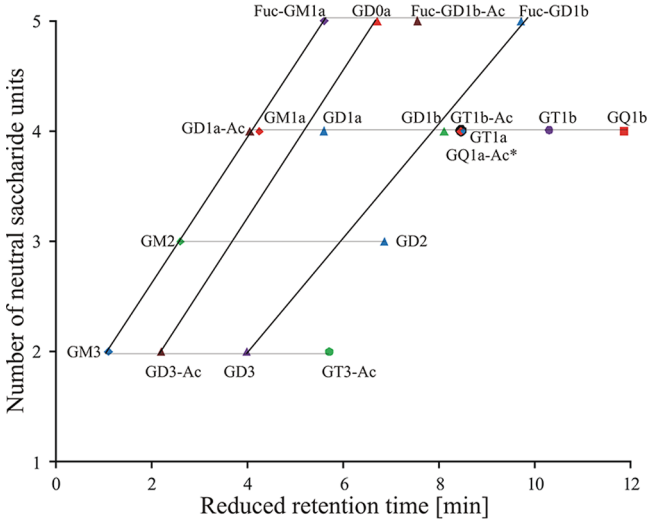

Figure 5. Dependence of reduced retention times in HILIC/ESI-MS on the number of neutral saccharide units. Annotation of gangliosides according to the number of sialic acids: GM, diamond; GD, triangle; GT, circle; and GQ, square. Abbreviations of gangliosides are depicted in Figure 1.

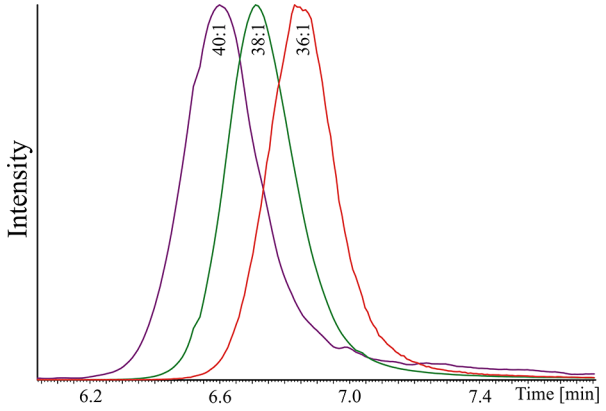

Figure 6. Overlay of RIC chromatograms of individual ganglioside species inside GD1a subclass with the number of carbon atoms and double bonds in fatty acyl chains.

studied gangliosides are present in one ionic form. The equilibrium of more charged forms should be avoided, because it may cause a peak tailing. Figure S-1 shows the calculated dissociation equilibria for GT1, GD1, and GM1. Only one triply charged form of GT1 is present in the pH range from 5 to 10 (Figure S-1A, red line). Negative charges are placed on carboxylates of three sialic groups in GT1. The neutral form is present at pH lower than 3 (Figure S-1A, blue line); however, it coexists with singly charged GT1 (yellow line, maximum at pH 2.4) and doubly charged GT1 (violet line, maximum at pH 3.2). Quadruply charged GT1 (green line) is predicted for pH higher than 10, where the addition charge is placed on the amino group of the *N*-acetylgalactosamine moiety. The similar interpretation can be described for GD1 (Figure S-1B) and GM1 (Figure S-1C), where the same region of pH from 5 to 10 corresponds to the single form for both GD1 (doubly charged, red line, Figure S-1B) and GM1 (singly charged, red line, Figure S-1C). Dissociation curves for *a*, *b*, and *c* series of

DOI: 10.1021/acs.analchem.7b03523
Anal. Chem. 2017, 89, 12425−12432

Table 1. Overview of Lipid Molecular Species Identified for Individual Lipid Subclasses in Porcine Brain, Human Kidney, Lungs, Plasma, and Erythrocyte Extracts Using HILIC/ESI−MS/MS Method

		sample type					
lipid subclass	retention time window [min]	porcine brain	human kidney	human lungs	human plasma	human erythrocytes	total
SulfoHexCer	0.6−1.7	38	25	3	2	4	43
SulfoHex$_2$Cer	0.6−1.7	-	25	-	-	4	25
PG	1.0−1.5	7	4	5	-	-	9
PI	1.0−1.5	10	20	13	8	9	20
LPI	1.7−2.4	8	8	4	5	-	10
PS	2.0−2.9	17	7	8	-	10	20
GM3	1.9−2.5	2	16	15	15	4	22
GD3-Ac	2.8−3.8	13	-	2	-	-	14
GM2	3.3−4.1	3	3	2	-	-	6
GD3	4.5−5.7	9	9	13	-	-	17
GD1a-Ac	4.8−5.5	3	-	-	-	-	3
GM1a	4.9−5.8	10	-	-	-	5	11
Fuc-GM1a	6.2−7.2	7	-	-	-	-	7
GD1a	6.3−7.1	7	4	2	-	-	10
GT3-Ac	6.3−7.3	6	-	-	-	-	6
GD0a	7.3−8.3	7	-	-	-	-	7
GD2	7.5−8.4	2	-	-	-	-	2
Fuc-GD1b-Ac	8.3−9.0	3	-	-	-	-	3
GD1b	8.8−9.6	8	-	-	-	-	8
GT1b-Ac	9.2−9.9	4	-	-	-	-	4
GQ1-Ac	9.2−9.9	2	-	-	-	-	2
GT1a	9.3−9.9	4	-	-	-	-	4
Fuc-GD1b	10.3−11.3	5	-	-	-	-	5
GT1b	10.8−12.0	12	-	-	-	-	12
GQ1b	12.4−13.5	2	-	-	-	-	2
total		189	122	67	30	36	272

ganglioside isomers are identical. The conclusion is that the optimal pH value should be in the range from 5 to 10.

Optimization of Buffer Composition. Based on the previous development of HILIC/ESI-MS method for acidic phospholipids,[33] Ascentis Si column has been tested for the separation of gangliosides. This column provides high efficiency for this type of acidic sphingolipids as well; therefore, it is further used in this work. The previous section describes the suggestion of optimal pH range based on theoretical calculations of dissociation equilibria, but it is essential to verify experimentally the best conditions for real separations. Moreover, the optimization of buffer type and concentration may have a critical importance, as known from our previous studies of acidic lipids.[33] The major ganglioside subclasses GM1a, Fuc−GM1a, GD1a, GD1b, and GT1b from the total ganglioside extract of porcine brain are used during the method development. Ammonium formate and acetate have been selected as volatile organic salts suitable for LC/MS operation in the concentration range from 0 to 30 mM (Figures 2, S-2, and Table S-1). The highest signal for ammonium formate or acetate is observed at 5 mM (Figure 2), but the best compromise between the sensitivity and peak shape is 10 mM. Mobile phases without any additives cannot be used for the separation due to the unacceptable peak tailing and no chromatographic resolution of isomeric GD1a and GD1b (Table S-1).

The pH range from 3.0 to 5.8 is tested for 10 mM of ammonium formate using the addition of formic acid (Figure S-3A and Table S-2) and from 3.0 to 6.5 for 10 mM of ammonium acetate using the addition of acetic acid (Figure S-3B and Table S-2). The direct comparison of optimum conditions for both tested buffers in Figure S-3C shows that the best results are obtained for ammonium acetate at pH 6.1. The peak width and tailing factors are illustrated in Figure S-4, Tables S-3 and S-4, where the worst results are obtained for most acidic mobile phases (pH 3) without any resolution of GD1a and GD1b. Measurements for all other pH values provide comparable results. Therefore, the best compromise among the sensitivity, tailing factors, and the chromatographic resolution is 10 mM of ammonium acetate, because it also provides a partial separation of Fuc−GM1a and GD1a unlike to 5 mM of ammonium acetate, but at cost of reduced sensitivity and longer analysis time, as shown in Figure S-5 with reconstructed ion current (RIC) chromatograms of GM1a, Fuc−GM1a, GD1a, GD1b, and GT1b.

Interpretation of MS/MS Spectra of Gangliosides. The application of the final method for the analysis of porcine brain extract is shown in Figure 3, where 19 ganglioside subclasses and 5 other polar lipid subclasses are detected. The full scan negative-ion ESI mass spectra are obtained for all peaks corresponding to individual subclasses of gangliosides, and the elemental composition is determined on the basis of accurate m/z measurements with the average mass accuracy of 3.1 ppm. Then, MS/MS spectra of $[M-H]^-$, $[M-2H]^{2-}$, or $[M-3H]^{3-}$ ions are recorded and interpreted. The charge state of precursor ion depends mainly on the number of sialic acids present in particular ganglioside. The fragmentation behavior of gangliosides (Figures 4 and S-6 to S-14) provides an excellent tool for sequencing of oligosaccharide part. The fragmentation is predictable and therefore provides unambiguous information on the sequence including the type of branching, i.e., the differentiation of *a*, *b*, and *c* series (see Figure 1).[5] All observed

DOI: 10.1021/acs.analchem.7b03523
Anal. Chem. 2017, 89, 12425−12432

fragment ions are singly charged with the only exception of m/z 931.5, which corresponds to $[M-2H-NeuAc_2]^{2-}$ ion in Figure S-12 or $[M-2H-NeuAc]^{2-}$ ion in Figures S-13 and S-14. The fragmentation of the most common gangliosides GM3, GM2, GM1a, and Fuc−GM1a has been well described in previous works.[18,34,35] The trace amount of GQ1a−Ac* does not allow the measurement of MS/MS spectra (labeled by asterisk), but the series *a* may be proposed on the basis of the characteristic retention behavior (Figure 5). The interpretation of MS/MS spectra of all other gangliosides subclasses (see structures in Figure 1) is described in the following figures: GD1a (Figure 4A), GD1b (Figure 4B), Fuc−GD1b (Figure 4C), Fuc−GD1b−Ac (Figure 4D), GD1a−Ac (Figure S-10), GD0a (Figure S-11), GT1b−Ac (Figure S-12), GQ1b (Figure S-13), GT1a (Figure S-14A), and GT1b (Figure S-14B). The symbol of black diamond highlights the precursor ions in MS/MS spectra.

Table S-5 lists characteristic neutral losses (NL) of individual saccharides units, and Table S-6 shows characteristic fragment ions related to the saccharide part of ganglioside molecules. There are several features in the fragmentation, which can be generally applied during the interpretation of unknown gangliosides. The fragmentation typically starts with the cleavage of sialic acids (NL of NeuAc, $\Delta m/z$ 291) until all sialic acids are lost. The Supporting Information is the presence of NeuAc fragment ion at m/z 290. The additional acetylation on the sialic acid ($NeuAc_2$) corresponds to the NL of $\Delta m/z$ 333 and the fragment ion $NeuAc_2$ at m/z 332. The position of $NeuAc_2$ can be determined according to the order of individual NL, as shown for example in Figure 4D. The presence of two or more neighboring sialic acids is identified on the basis of abundant characteristic fragment ions, such as NeuAc−NeuAc (m/z 581, Figure 4B,C), NeuAc−$NeuAc_2$ (m/z 623, Figure 4D), and NeuAc−NeuAc−$NeuAc_2$ (m/z 914, Figure S-9). The relative abundance of $[M-2H-2NeuAc]^-$ ion at m/z 1253.8 is higher in case of *b* series (Figure 4B), because it requires the cleavage of only one bond unlike to *a* series (Figure 4A), where two bonds have to be cleaved to obtain this fragment ion. The unambiguous proof of *b* series is the presence of abundant ion of NeuAc−NeuAc at m/z 581 in Figure 4B. This way the sequence of all sialic acids can be unambiguously assigned, which determines the series *a*, *b*, and *c* (see Figure 1). The further proof is the characteristic chromatographic behavior described in the next chapter. The presence of terminal fucose is recognized by the characteristic NL of $\Delta m/z$ 146 and also the fragment ion Fuc−Hex−HexNAc at m/z 510 (Figure 4C,D). The total fatty acyl composition in the ceramide part is indicated by characteristic fragment ions, such as m/z 564 for 36:1, m/z 592 for 38:1, and so on.

The identification of polar phospholipids and sulfatides follows well-known rules described in our previous works.[30,36−38] In case of sulfatides, frequent mass interferences occur for sulfatide species with the additional hydroxyl group (e.g., SulfoHexCer 38:2 (OH) at m/z 848.5563) vs sulfatides with the additional methylene group and one double bond less (e.g., SulfoHexCer 39:1 at m/z 848.5927). These species cannot be resolved by the resolving of our QTOF, which causes lower mass accuracy for these doublets, but the identification of all reported species is still clearly confirmed by the their fragmentation and retention behavior.

Retention Behavior of Gangliosides in HILIC Mode. The retention behavior of lipids follow the regular patterns related to the type of polar headgroup, the number of carbon atoms in fatty acyl chains and also the number of double bonds, as illustrated in numerous previous works.[21,29,30,33,39,40] Regularities in lipid retention behavior can be used for the prediction of retention times and then applied as an additional Supporting Information for the lipid identification. This approach is applicable both in reversed-phase[21,29,39] and HILIC[16,30,33,40] modes and recently in ultrahigh-performance supercritical fluid chromatography as well,[36] and therefore, the similar approach is tested for gangliosides with higher structural complexity caused by the presence of oligosaccharide part. Figure 5 shows the dependence of reduced retention times of gangliosides on the number of saccharide units with fitting of some observed logical series in this graph, for example, the series of GM3, GM2, GM1a, and Fuc−GM1a (see structures in Figure 1) shows an excellent fit. Higher number of saccharide units results in higher retention with the increment of approximately 1.5−3 min, but it depends on the type of saccharide units. This increase is about 1.5 min for the fucosylation, but the difference between GD3 and GD2 is up to 3 min. The same behavior is observed for sialic acids, where higher number of sialic acids strongly increases the retention by about 3.5−4 min. The retention of *a* series is 2−3 min lower in comparison to *b* series, which enables the assignment of *a* series in case of GQ1a−Ac*, which is the only ganglioside subclass without MS/MS due to very low concentration. The additional acetylation on the sialic acid ($NeuAc_2$) corresponds to the lower retention by slightly less than 2 min.

In HILIC mode, the partial separation inside peaks of individual ganglioside subclasses can be detected using the overlay of RIC chromatograms similarly as for other lipid subclasses investigated earlier.[16,30,36] The retention slightly decreases with increasing length of fatty acyls (Figures 6), which is the additional information for the structure confirmation.

LC/MS Analysis of Biological Samples. The final method is applied for measurements of human kidney, lungs, plasma, erythrocytes, and porcine brain extracts. The full list of all identified gangliosides and other polar lipid subclasses (phosphatidylserines (PS), phosphatidylinositols (PI), lyso-phosphatidylinositols (LPI), phosphatidylglycerols (PG), and sulfatides (SulfoHexCer)) is shown in Table S-7 with their relative intensities determined from RIC of individual species within particular subclasses together with mass accuracies. Only gangliosides that are identified with high confidence are reported here considering the following criteria: (1) accurate m/z values to determine the elemental composition (99% of measurements <10 ppm, 87% of measurements <5 ppm, and the average mass accuracy 3.1 ppm), (2) the interpretation of fragmentation behavior to sequence the oligosaccharide part of the molecule based on accurate m/z values, and (3) retention times in accordance with the predicted retention behavior shown in Figure 5. The previously reported information on the fragmentation behavior of gangliosides[5,18] is in agreement with our observations as well. The overview in Table 1 and the full list in Table S-7 clearly show that the brain tissue contains by far more gangliosides than other studied biological samples. Only GM3 is detected for all studied sample types with only few additional gangliosides in case of kidney (3 GD3−Ac, 3 GM2, 9 GD3, and 4 GD1a), lungs (2 GM2, 10 GD3, and 2 GD1a), and erythrocytes (4 GM1a).

DOI: 10.1021/acs.analchem.7b03523
Anal. Chem. 2017, 89, 12425−12432

CONCLUSIONS

Our new HILIC/ESI-MS/MS approach enables unambiguous identification of the highest number of gangliosides ever reported for studied biological samples. HILIC separation has been well-optimized, which results in the characterization of 145 ganglioside molecular species from 19 subclasses with additional identification of other 6 polar lipid subclasses (SulfoHexCer, SulfoHex$_2$Cer, PG, PI, LPI, and PS), which are known to be difficult for established MS-based lipidomic platforms. The identification of gangliosides and other lipids is based on high-resolution MS measurements providing high mass accuracy for both precursor and product ions, the agreement of fragmentation behavior in MS/MS with structure assignment, the correlation with the predicted retention behavior of ganglioside subclasses and also ganglioside species inside the individual subclass. The combination of this complementary information provides highly confident identification. The next step is the change of this qualitative method into the quantitative workflow using suitable internal standards and the method validation with application to real clinical samples. The present HILIC/ESI-MS is already optimized in terms of future planned quantitative high-throughput analysis, because the analysis time is fast, can be easily automated, and the lipid subclass separation is the best available approach for the lipidomic quantitation.

ASSOCIATED CONTENT

Supporting Information

The Supporting Information is available free of charge on the ACS Publications website at DOI: 10.1021/acs.analchem.7b03523.

Dissociation equilibria, comparison of peak widths, tailing factors, and relative peak areas at different mobile-phase composition, effect of ammonium acetate concentration on the separation, fragmentation behavior, characteristic neutral losses and fragment ions for individual ganglioside subclasses, list of lipids identified in porcine brain, human kidney, lungs, plasma, and erythrocytes (PDF)

AUTHOR INFORMATION

Corresponding Author

*Tel.: +420-466037087; Fax: +420-466037068; E-mail: Michal.Holcapek@upce.cz.

ORCID

Michal Holčapek: 0000-0003-3978-1249

Notes

The authors declare no competing financial interest.

ACKNOWLEDGMENTS

This work was supported by the ERC CZ grant project LL1302 sponsored by the Ministry of Education, Youth and Sports of the Czech Republic. Authors would like to thank Bohuslav Melichar and David Vrána (Palacky University, Medical School and Teaching Hospital, Department of Oncology, Olomouc, Czech Republic) for providing biological samples.

REFERENCES

(1) Fahy, E.; Subramaniam, S.; Brown, H. A.; Glass, C. K.; Merrill, A. H.; Murphy, R. C.; Raetz, C. R.; Russell, D. W.; Seyama, Y.; Shaw, W.; et al. *J. Lipid Res.* **2005**, *46*, 839−862.

(2) Aureli, M.; Mauri, L.; Ciampa, M. G.; Prinetti, A.; Toffano, G.; Secchieri, C.; Sonnino, S. *Mol. Neurobiol.* **2016**, *53*, 1824−1842.

(3) Schauer, R. *Zoology* **2004**, *107*, 49−64.

(4) Malykh, Y. N.; Schauer, R.; Shaw, L. *Biochimie* **2001**, *83*, 623−634.

(5) Ikeda, K.; Taguchi, R. *Rapid Commun. Mass Spectrom.* **2010**, *24*, 2957−2965.

(6) Lacomba, R.; Salcedo, J.; Alegría, A.; Lagarda, M. J.; Barberá, R.; Matencio, E. *J. Pharm. Biomed. Anal.* **2010**, *51*, 346−357.

(7) Giuffrida, F.; Elmelegy, I. M.; Thakkar, S. K.; Marmet, C.; Destaillats, F. *Lipids* **2014**, *49*, 997−1004.

(8) Ma, L.; MacGibbon, A. K.; Mohamed, H. J. B. J.; Loy, S.; Rowan, A.; McJarrow, P.; Fong, B. Y. *Int. Dairy J.* **2015**, *49*, 62−71.

(9) Fuller, M.; Duplock, S.; Hein, L. K.; Rigat, B. A.; Mahuran, D. J. *Anal. Biochem.* **2014**, *458*, 20−26.

(10) Valdes-Gonzalez, T.; Goto-Inoue, N.; Hirano, W.; Ishiyama, H.; Hayasaka, T.; Setou, M.; Taki, T. *J. Neurochem.* **2011**, *116*, 678−683.

(11) Sonnino, S.; Mauri, L.; Ciampa, M. G.; Prinetti, A. *J. Neurochem.* **2013**, *124*, 432−435.

(12) Sonnino, S.; Mauri, L.; Chigorno, V.; Prinetti, A. *Glycobiology* **2007**, *17*, 1R−13R.

(13) Lopez, P. H.; Schnaar, R. L. *Curr. Opin. Struct. Biol.* **2009**, *19*, 549−557.

(14) Hakomori, S.-I. *J. Biol. Chem.* **1990**, *265*, 18713−18716.

(15) Hakomori, S.-I.; Handa, K. *Glycoconjugate J.* **2015**, *32*, 1−8.

(16) Cífková, E.; Holčapek, M.; Lísa, M.; Ovčačíková, M.; Lyčka, A.; Lynen, F.; Sandra, P. *Anal. Chem.* **2012**, *84*, 10064−10070.

(17) Garcia, A. D.; Chavez, J. L.; Mechref, Y. *J. Chromatogr. B: Anal. Technol. Biomed. Life Sci.* **2014**, *947-948*, 1−7.

(18) Ikeda, K.; Shimizu, T.; Taguchi, R. *J. Lipid Res.* **2008**, *49*, 2678−2689.

(19) Prinetti, A.; Rocchetta, F.; Costantino, E.; Frattini, A.; Caldana, E.; Rucci, F.; Bettiga, A.; Poliani, P. L.; Chigorno, V.; Sonnino, S. *Glycoconjugate J.* **2009**, *26*, 623−633.

(20) Tsui, Z.-C.; Chen, Q.-R.; Thomas, M. J.; Samuel, M.; Cui, Z. *Anal. Biochem.* **2005**, *341*, 251−258.

(21) Hu, T.; Jia, Z.; Zhang, J. *Anal. Chem.* **2017**, *89*, 7808−7816.

(22) Sarbu, M.; Robu, A. C.; Ghiulai, R. M.; Vukelić, Z.; Clemmer, D. E.; Zamfir, A. D. *Anal. Chem.* **2016**, *88*, 5166−5178.

(23) Sarbu, M.; Robu, A. C.; Ghiulai, R. M.; Vukelić, Z.; Clemmer, D. E.; Zamfir, A. D. *Anal. Chem.* **2016**, *88*, 5166−5178.

(24) Fong, B.; Norris, C.; Lowe, E.; McJarrow, P. *Lipids* **2009**, *44*, 867−874.

(25) Huang, Q.; Liu, D.; Xin, B.; Cechner, K.; Zhou, X.; Wang, H.; Zhou, A. *Anal. Chim. Acta* **2016**, *929*, 31−38.

(26) Dufresne, M.; Guneysu, D.; Patterson, N. H.; Marcinkiewicz, M. M.; Regina, A.; Demeule, M.; Chaurand, P. *Anal. Bioanal. Chem.* **2017**, *409*, 1425−1433.

(27) Škrášková, K.; Claude, E.; Jones, E. A.; Towers, M.; Ellis, S. R.; Heeren, R. M. *Methods* **2016**, *104*, 69−78.

(28) Folch, J.; Lees, M.; Sloane-Stanley, G. *J. Biol. Chem.* **1957**, *226*, 497−509.

(29) Ovčačíková, M.; Lísa, M.; Cífková, E.; Holčapek, M. *J. Chromatogr. A* **2016**, *1450*, 76−85.

(30) Cífková, E.; Holčapek, M.; Lísa, M. *Lipids* **2013**, *48*, 915−928.

(31) Svennerholm, L. *J. Neurochem.* **1963**, *10*, 613−623.

(32) Chester, M. *Eur. J. Biochem.* **1998**, *257*, 293.

(33) Cífková, E.; Hájek, R.; Lísa, M.; Holčapek, M. *J. Chromatogr. A* **2016**, *1439*, 65−73.

(34) Fong, B. Y.; Ma, L.; Khor, G. L.; van der Does, Y.; Rowan, A.; McJarrow, P.; MacGibbon, A. K. *J. Agric. Food Chem.* **2016**, *64*, 6295−6305.

(35) Domon, B.; Costello, C. E. *Glycoconjugate J.* **1988**, *5*, 397−409.

(36) Lísa, M.; Holčapek, M. *Anal. Chem.* **2015**, *87*, 7187−7195.

(37) Lísa, M.; Cífková, E.; Holčapek, M. *J. Chromatogr. A* **2011**, *1218*, 5146−5156.

(38) Jirásko, R.; Holčapek, M.; Khalikova, M.; Vrána, D.; Študent, V.; Prouzová, Z.; Melichar, B. *J. Am. Soc. Mass Spectrom.* **2017**, *28*, 1562−1574.

DOI: 10.1021/acs.analchem.7b03523
Anal. Chem. 2017, 89, 12425−12432

(39) Fauland, A.; Köfeler, H.; Trötzmüller, M.; Knopf, A.; Hartler, J.; Eberl, A.; Chitraju, C.; Lankmayr, E.; Spener, F. *J. Lipid Res.* **2011**, *52*, 2314−2322.
(40) Cífková, E.; Holčapek, M.; Lísa, M.; Vrána, D.; Gatěk, J.; Melichar, B. *Anal. Bioanal. Chem.* **2015**, *407*, 991−1002.

DOI: 10.1021/acs.analchem.7b03523
Anal. Chem. 2017, 89, 12425−12432